Electrochemical and Solid-State Letters, **5** (4) C49-C52 (2002)
0013-4651/2002/5(4)/C49/4/$7.00 © The Electrochemical Society, Inc.

Superconformal Electrodeposition in Vias

D. Josell,[z] D. Wheeler, and T. P. Moffat*

National Institute of Standards and Technology, Metallurgy Division, Gaithersburg, Maryland 20899, USA

Conditions for which superconformal filling of vias can be expected are predicted using the curvature enhanced accelerator coverage mechanism to model the effect of accelerator accumulation and area change on local copper deposition rate. Superconformal filling of vias is predicted to occur over a more limited range of electrodeposition conditions than in trenches of similar aspect ratio with significant implications for dual damascene processing. Parameters for the model describing both the accumulation of accelerator on the copper/electrolyte interface and the impact of the accumulated accelerator on the local deposition rate come from voltammetry experiments on planar electrodes. An idealized geometry permits reduction of the 3D filling problem to solution of a system of coupled first-order, nonlinear ordinary differential equations.
© 2002 The Electrochemical Society. [DOI: 10.1149/1.1452485] All rights reserved.

Manuscript submitted September 21, 2001; revised manuscript received December 4, 2001. Available electronically February 6, 2002.

Dual-damascene processing of semiconductor devices involves simultaneous electrodepositon of copper for both trenches and vias. Until recently, such processing has proceeded both with proprietary operational parameters and in the absence of a robust physical description of the feature filling process. This combination of factors has slowed scientific assessment of future prospects for this technology.

Modeling of via filling in particular has been limited. One study detailed the effects of geometry on cupric ion depletion in an additive free electrolyte.[1] That study did not address superconformal filling (*i.e.*, superfilling), which requires the use of both deposition rate inhibiting and accelerating additives in the electrolyte. Early models of superfilling assumed location-dependent growth rates derived from diffusion limited accumulation of only an inhibiting species in trenches[2] and vias.[3] Such models were unable to predict several key experimental observations of filling, including the initial period of conformal growth, general fill geometry during superconformal filling, and subsequent development of an overfill bump.[4-7] Recently, however, modeling has advanced significantly with the publication of both a model electrolyte for the study of superconformal electrodeposition[7] and a curvature enhanced accelerator coverage (CEAC) mechanism that permits a quantitative description of superconformal deposition in trenches.[8,9]

The first part of the mechanism is that a dilute accelerating species (thiol or disulfide derived from a 3-mercapto-1-propanosulfonate additive (MPSA)) adsorbs strongly on the depositing metal surface, thereby displacing the more weakly bound inhibiting species (derived from polyethylene glycol and chloride (PEG-Cl) additives). All adsorbed species are presumed to remain on or float at the surface during deposition. The second part of the mechanism involves the compression of adsorbed accelerator with reduction of surface area during growth, such as occurs at points of high positive curvature like the bottoms of small vias, resulting in increased local velocity. Models based on the CEAC mechanism have been shown to yield predictions that agree well with experimental results, including a period of conformal growth, bottom-up filling or void formation, and creation of overfill bumps, for filling of trenches between ~350 and 100 nm wide and 500 nm deep over a wide range of processing conditions.[8-11]

One such model used an idealized geometry and simplified cupric depletion to reduce the trench filling problem to a first-order ordinary differential equation that could predict the potential and concentration dependence of filling over a range of aspect ratios (height/width).[11] Predictions were compared with experimental results as well as results of a model that solves for the space and time dependent cupric ion and accelerator concentrations in the electrolyte using the actual interface shape.[9,10] Agreement was good in both cases for the range of parameter space studied.

This work is the first to extend a model that successfully predicts all aspects of trench filling, in this case a CEAC-based model, to superconformal filling of vias. The time-dependent copper/electrolyte interface shape is approximated by a cylinder for the side wall of the via and a plane for the bottom, and a cupric ion concentration varying linearly with distance down the via is assumed. The CEAC mechanism is then applied to the via geometry. Superconformal deposition by the CEAC mechanism might be anticipated to be enhanced as compared to that for trenches because the bottoms of vias have two nonzero radii of curvature while the bottoms of trenches have only one. However, unlike the sidewalls of trenches, the sidewalls of vias have nonzero curvature. This causes deposition on the sidewalls of vias to also be affected (accelerated) by the CEAC mechanism, to the detriment of superfilling.

Model

Determining the equations of evolution.—The time dependent interface shape of the copper/electrolyte interface is approximated for all times by a cylindrical surface, shown schematically in Fig. 1. The validity of this approximation (and other approximations to come) has been discussed previously in the context of filling of trenches.[11] Filling of a via of initial radius R and height h is monitored by tracking the motion of the bottom and side surfaces. The velocity v is given by

$$v(\theta,C,\eta) = \frac{C}{C_{\mathrm{Cu}}} v_{\mathrm{o}}(\theta) \exp\left(-\frac{\alpha(\theta)F}{R_{\mathrm{B}}T}\eta\right) \qquad [1]$$

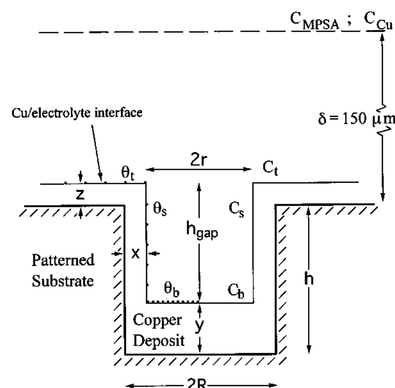

Figure 1. A schematic of the idealized geometry used to model filling of vias, viewed as a cross section through the midplane.

* Electrochemical Society Active Member.
[z] E-mail: daniel.josell@nist.gov

with $F = 96{,}485$ C/mol, $R_B = 8.314$ J/mol K, and $T = 293$ K, surface coverage of accelerator θ, overpotential η, and cupric ion concentrations C_{Cu} (2.5×10^{-4} mol/cm^3) in the bulk electrolyte and C at the interface.[7-9] All parameters are obtained from the results of cyclic voltammetry (CV) on planer substrates with the understanding that $v = i(\theta)\Omega_{Cu}/2F$, with $i(\theta)$ the current density and Ω_{Cu} the atomic volume of copper. The accumulation of accelerator from the electrolyte to the surface is approximated to have no explicit spatial variation within the feature. It is expressed in terms of the concentration of the additive in the bulk electrolyte C_{MPSA}, the diffusion coefficient D_{MPSA}, the number of available sites $\Gamma(1-\theta)$, and a potential dependent rate constant $k(\eta)$ by[9]

$$\frac{d\theta_t}{dt} = \frac{C_{MPSA}k(1-\theta_t)}{1+\delta\Gamma k(1-\theta_t)/D_{MPSA}} \qquad [2]$$

where $k = 1.8 \times 10^5$ to $2.7 \times 10^7\ \eta^3$ [cm^3/mol s], $D_{MPSA} = 1 \times 10^{-5}$ cm^2/s, the thickness of the boundary layer is $\delta = 150$ μm, the areal density of absorption sites is $\Gamma = 9.7 \times 10^{-10}$ mol/cm^2 and accumulation is zero at zero time, $\theta_t(0) = 0$. Equation 2, with parameters also obtained by CV on planer substrates, captures the gradient of concentration across the boundary layer as well as the equality of the fluxes diffusing across the boundary layer and attaching to the interface. With the rate thus defined, the accelerator accumulated on the interface saturates at unity coverage (one monolayer). As done previously,[8-11] a value of $\theta = 1$ is used when shrinking area would make θ rise above unity. Excess is thus implicitly destroyed or incorporated into the deposited copper. Consumption of the adsorbed accelerator is ignored, an approximation that has been shown to be a reasonable estimate of actual consumption during copper deposition for the time scales relevant to feature filling.[12]

For potentiostatic deposition (fixed η), the radial displacements of the sidewalls, x, is expressed in terms of the accelerator coverage θ_s and the local cupric ion concentration C_s

$$r(t) = R - x(t) = R - \int_0^t v(\theta_s(t), C_s(t))dt \equiv R - \int_0^t v_s(t)dt \qquad [3]$$

The vertical displacement of the bottom surface is expressed in terms of the accelerator coverage θ_b and the local cupric ion concentration C_b

$$y(t) = \int_0^t v(\theta_b(t), C_b(t))dt \equiv \int_0^t v_b(t)dt \qquad [4]$$

The vertical displacement of the top surface is expressed in terms of the accelerator coverage θ_t and the local cupric ion concentration C_t,

$$z(t) = \int_0^t v(\theta_t(t), C_t(t))dt \equiv \int_0^t v_t(t)dt \qquad [5]$$

The coverage of accelerator on the sidewalls, $\theta_s(t)$, is postulated to follow

$$\frac{d\theta_s}{dt} = \frac{C_{MPSA}k(1-\theta_s)}{1+\delta\Gamma k(1-\theta_s)/D_{MPSA}} + \frac{\theta_s v_s}{R-x} \qquad [6]$$

The first term accounts for accumulation from the electrolyte. It is identical in form to the expression for accumulation of accelerator on the top surface as expressed in Eq. 2 because depletion of accelerator down the via is assumed to be negligible. The second term accounts for coverage increase caused by the area change due to the shrinking radius of the unfilled volume of the via; this is the CEAC mechanism. As no accelerator has accumulated at zero time, $\theta_s(0) = 0$. The coverage on the bottom surface, $\theta_b(t)$, is postulated to follow

$$\frac{d\theta_b}{dt} = \frac{C_{MPSA}k(1-\theta_b)}{1+\delta\Gamma k(1-\theta_b)/D_{MPSA}} + \frac{2\theta_s v_b}{R-x} + \frac{2\theta_b v_s}{R-x} \qquad [7]$$

The first term again represents the accumulation from the electrolyte. The last two terms represent accrual of the accelerator that was on the sidewall region eliminated by the upward motion of the bottom surface and concentration associated with the shrinking bottom surface area, respectively (Fig. 1). As in the simple model for trench filling,[11] Eq. 6 and 7 implicitly assume accelerator on the sidewall area eliminated by the upward moving bottom surface is distributed uniformly on the bottom surface. Again, $\theta_b(0) = 0$. Equations 6 and 7 are nonlinear first-order differential equations in θ_s and θ_b. They can be solved using the experimentally derived kinetic parameters and Eq. 1.

From Eq. 3, the time t^* at which the sidewalls would reach the center of the via (Fig. 1), is defined by

$$x(t^*) \equiv R \qquad [8]$$

The criterion for filling is that the bottom surface reaches the top of the via before the sides impinge leaving a seam (or void). From Fig. 1, this can be written as

$$y(t^*) \geqslant h \qquad [9]$$

with t^* determined from Eq. 8 and $y(t)$ from Eq. 4. The equality holds at the transition between conditions that lead to fill *vs.* those that lead to formation of a seam (or void). The conditions for fill are now expressed in terms of the functions $\nu(\theta, C, \eta)$ and the geometrical consequences of growth in the via in Eq. 6 and 7. The evolution of the quantities $\theta_b(t)$, $\theta_s(t)$, $\theta_t(t)$, $v_b(t)$, $v_s(t)$, and $v_t(t)$, and thus $y(t)$ and $x(t)$ for Eq. 8 and 9, can be numerically evaluated using Eq. 1-7 once the cupric ion concentrations $C_b(t)$, $C_s(t)$, and $C_t(t)$ are known.

Accounting for cupric ion depletion.—The impact of cupric ion Cu^{2+} depletion both across the boundary layer and down the via itself is determined as follows. Balancing the copper ion flux at the top of the gap (see Fig. 1) with the copper consumed through motion of the sidewalls and bottom gives

$$r\Omega_{Cu}D_{Cu}\nabla C|_{top} = 2h_{gap}v_s + rv_b \qquad [10]$$

with cupric ion diffusion coefficient $D_{Cu} = 5 \times 10^{-6}$ cm^2/s and $\Omega_{Cu} = 7.1$ cm^3/mol. In keeping with the approximate nature of the solution, Eq. 10 assumes that the cupric deposition rate on the sidewall region above the original via equals that within the via (coverage given by Eq. 6); this ignores the fact that the sidewall above the via is newer and thus has had less time to accumulate accelerator. The ∇C is approximated as constant down the via; consistent with the composition gradient, cupric ion consumption by the sidewalls is modeled as occurring at the bottom of the via. For time-dependent concentrations of cupric ion at the bottom (C_b) and top (C_t) of the via related by

$$C_b(t) \equiv \beta C_t(t) \qquad [11]$$

with $\beta(t) \leqslant 1$ during deposition, Eq. 10 can be rewritten

$$r\Omega_{Cu}D_{Cu}\frac{C_t(1-\beta)}{h_{gap}} = 2h_{gap}v_s + rv_b \qquad [12]$$

For the conditions studied here, the diffusion field over the (isolated) via is treated as that above a planar surface, rather than the hemispherical solution, in order to model a limited patterned region and convection within the boundary layer.[9,11] The concentration of

cupric ion at the top of the via C_t can then be written in terms of the bulk concentration C_{Cu} in the electrolyte by equating the flux of cupric ions diffusing across the boundary layer and the copper incorporation into the top surface, moving at velocity $v_t(t)$, to obtain

$$C_t(t) = C_{Cu} - \frac{\delta v_t}{\Omega_{Cu} D_{Cu}} \quad [13]$$

The time-dependent decrease of C_t below the bulk value C_{Cu} reflects the concentration drop across the boundary layer required to supply the increasing cupric ion consumption associated with the increasing surface coverage of accelerator. Approximating the cupric ion concentration for the sidewalls (C_s) as equal to that at the top of the via (C_t), to obtain an upper bound on sidewall velocity, gives

$$C_s(t) = C_{Cu} - \frac{\delta v_t}{\Omega_{Cu} D_{Cu}} \quad [14]$$

This approximation models void formation by more rapid sidewall growth near the top of the via where there is less cupric ion depletion. Using Eq. 12 and 13 and $h_{gap} = h + z - y$ and $r = R - x$ (see Fig. 1) one can obtain

$$\beta(t) = 1 - \frac{(h + z - y)}{(R - x)} \frac{[2(h + z - y)v_s + (R - x)v_b]}{(C_{Cu}\Omega_{Cu}D_{Cu} - \delta v_t)} \quad [15]$$

Finally, Eq. 11, 13, and 15 yield

$$C_b(t) = \left(1 - \frac{(h + z - y)}{(R - x)} \frac{[2(h + z - y)v_s + (R - x)v_b]}{(C_{Cu}\Omega_{Cu}D_{Cu} - \delta v_t)}\right) \times \left(C_{Cu} - \frac{\delta v_t}{\Omega_{Cu} D_{Cu}}\right) \quad [16]$$

This concentration reflects the concentration drop across the boundary layer as well as down the via itself.

The cupric concentrations C_t, C_s, and C_b expressed in terms of the velocities v_b, v_s, and v_t (Eq. 13, 14, and 16) with the empirical formulas $v_s(C_s)$, $v_b(C_b)$, and $v_t(C_t)$ in Eq. 3, 4, and 5 (the functional form $v(C)$ in Eq. 1), provide six nonlinear equations that are solved for the six unknowns C_t, C_s, C_b, v_t, v_s, and v_b. With Eq. 2, 6, and 7 defining the impact of the growth rates v_t, v_s, and v_b on the evolution of the surface coverages θ_t, θ_s, and θ_b, the equations describing via filling in the simple model are now fully determined.

Predictions of the Model

Figure 2 shows model predictions, specifically whether fill or fail is to be expected, for the experimentally derived velocity function[9]

$$v(\theta,\eta,C) = \frac{\Omega_{Cu}}{2F}\frac{C}{C_{Cu}}(0.069 + 0.64\theta) \times \exp\left(-\frac{(0.447 + 0.299\theta)F}{R_B T}\eta\right) \quad [17]$$

with the remaining parameters as given earlier. The via depth h used for the fill criterion in Eq. 8 is 0.5 μm; this value is used for all modeling. The curves delineate the border between fill *vs.* fail conditions for a series of deposition voltages. The existence of an optimal range of accelerator concentrations C_{MPSA} can be understood through the model. Too low a value leads to inadequate coverage θ_b and inadequate upward acceleration of the bottom surface, even with geometrical compression. Too high a value leads to near-unity coverage θ_s (as well as θ_b) and thus equal, albeit high, velocities for all surfaces (conformal growth). The generally improved filling with overpotential η going from −0.14 to −0.26 V is associated with the increase of the ratio $v(\theta = 1)/v(\theta = 0)$ with increasing overpotential η that was noted earlier. The maximization (at an aspect ratio greater than five) and subsequent decrease (not shown) of predicted fill conditions at overpotentials beyond −0.28 V result from higher deposition rates that increase cupric depletion within the via and decrease time for accumulation of accelerator. The maximum fillable aspect ratio is predicted to decrease by 0.12 per μmol/L for C_{MPSA} twice the optimal ≈2 μmol/L at $\eta = -0.2$ V (Fig. 2). For comparison, the maximum fillable aspect ratio of a trench is predicted to decrease by only 0.06 per μmol/L for C_{MPSA} twice the optimal ≈10 μmol/L at $\eta = -0.2$ V.[11] This enhanced sensitivity of via filling to electrolyte concentration is caused by acceleration of deposition on the sidewalls that follows the acceleration of deposition on the bottom, restricting the window for superfilling.

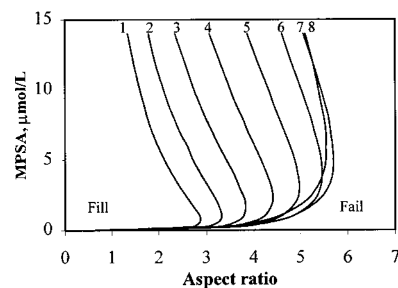

Figure 2. Fill/fail boundaries predicted by the model as a function of the concentration of accelerator in the electrolyte are shown for representative overpotentials. Curves are enumerated according to overpotential in −0.02 V increments, *i.e.*, (1) −0.14, (2) −0.16, (3) −0.18, (4) −0.20, (5) −0.22, (6) −0.24, (7) −0.26, and (8) −0.28 V. Fill occurs at lower aspect ratios (left of appropriate fill/fail boundary), and failure to fill occurs at higher aspect ratios (right of appropriate boundary).

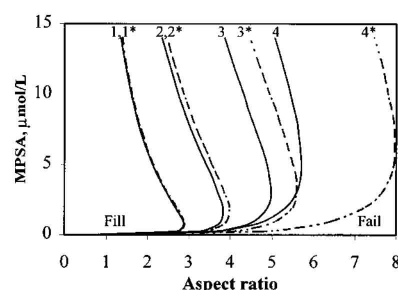

Figure 3. Fill/fail boundaries predicted by the simple model as a function of the concentration of accelerator in the electrolyte are shown for representative overpotentials. Solid curves are predicted including cupric depletion down the via while dashed curves ignore it. Curves are enumerated according to overpotential, with stars for the curves ignoring cupric depletion: (1 and 1*) −0.14, (2 and 2*) −0.18, (3 and 3*) −0.22, (4 and 4*) −0.26 V. The impact of cupric depletion on predicted filling of vias is most significant at the higher deposition rates associated with the larger overpotentials.

These results are generally conservative because sidewall velocity obtained using the higher cupric concentration at the top of the via leads to more rapid sidewall closure (failure) as well as overestimation of cupric depletion down the via. Aggressive predictions can be obtained by letting $C_b = C_s = C_t$ as given by Eq. 13, thus accounting for cupric depletion across the boundary layer but not down the via itself. Figure 3 compares predictions in this case with those obtained when cupric depletion down the via is included (from Fig. 2). The predictions are very similar at lower overpotentials, *e.g.*, −0.14 and −0.18 V, where lower deposition rates are associated with minimal cupric depletion. For overpotentials as large as −0.26 V, it is evident that prediction of the fill/fail boundary requires accurate modeling of cupric ion consumption.

Predicted growth contours during filling of a 0.5 μm deep via with aspect ratio of 5 (height/width) are shown in Fig. 4a for addi-

tive concentration 5 μmol/L and overpotential −0.282 V. Figure 4b shows the corresponding histories of y and x, the copper deposition thickness from the via bottom and sides, respectively. Filling is indicated by the fact that y reaches the via height (0.5 μm) before x reaches the via radius. Figure 4c shows the corresponding histories of the accelerator coverages θ_b and θ_s, and Fig. 4d shows the corresponding histories of the cupric ion concentrations C_b and C_s. It is evident from Fig. 4b that nearly 90% of the y displacement of (*i.e.*, metal deposition on) the bottom surface occurs in the last few seconds, after accelerator coverage there has saturated (Fig. 4c). Accelerator coverage and metal deposition rate on the sidewalls are predicted to increase significantly shortly after those on the bottom surface (Fig. 4b and 4c). In contrast, rapid acceleration of metal deposition on the sidewalls of trenches is neither observed nor expected as trenches have no curvature to enhance accelerator coverage through the CEAC mechanism. The general decrease in cupric ion concentrations (Fig. 4d) is caused by the increasing deposition rates on all surfaces associated with the accumulation of the accelerator (Fig. 4c). The rapid decrease of C_b at ~12 s (Fig. 4d) is caused by the increasing gradient of concentration required to supply the accelerating deposition rate on the bottom surface. The sudden change of slope at ~13 s (Fig. 4d) is caused by attainment of $\theta_b = 1$ (Fig. 4c); with cupric consumption nearly maximized, the gap height over which the gradient exists rapidly decreases and the cupric concentration C_b approaches C_t $(=C_s)$.[11]

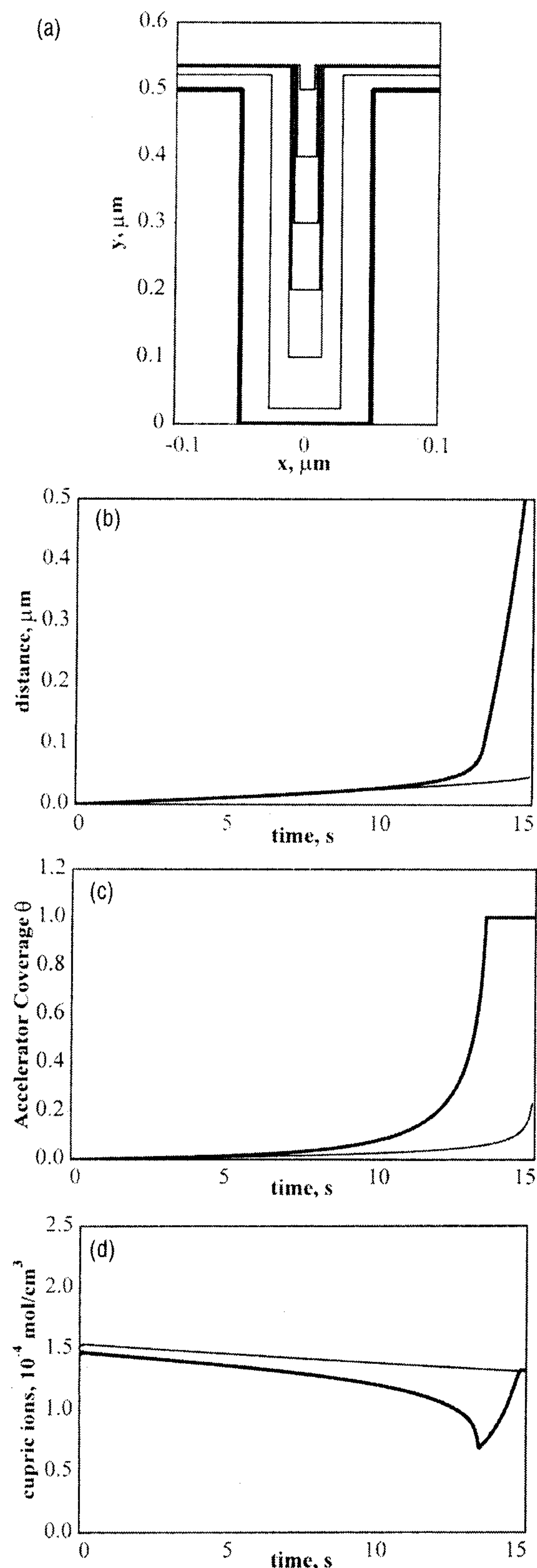

Figure 4. (a). Filling contours predicted by the simple model for C_{MPSA} = 5 μmol/L and η = −0.282 V. The via is 0.5 μm deep with aspect ratio of 5 (height/width). Data associated with the simulation: (b) The corresponding histories of the copper deposition thicknesses y and x, from the via bottom (thick line) and sides, respectively. The corresponding histories of θ_b and θ_s, the accelerator coverages on the bottom interface (thick line) and side interfaces, respectively. (d) The corresponding histories of C_b (thick line) and C_s, the cupric ion concentrations at the bottom and sidewalls, respectively, of the unfilled region.

Conclusions

This work presents the first predictions of filling of vias by superconformal electrodeposition. The CEAC mechanism is utilized to model the effect of accelerator accumulation and area change on local copper deposition rate to predict conditions for which fill can be expected. A simplified geometry permits reduction of the 3D filling problem to solution of a system of coupled differential equations. Calculations are made both with and without cupric depletion down the via to obtain conservative and aggressive bounding curves for the actual boundaries between filling and nonfilling conditions. Under optimal conditions, superfilling is predicted to occur in features with aspect ratios greater than five. Use of higher cupric ion concentrations can push this value higher. However, the optimal electrolyte composition is quite different than that for superfilling of trenches, which will reduce the aspect ratios of features that can be filled in dual damascene processing.

The National Institute of Standards and Technology assisted in meeting the publication costs of this article.

References

1. A. C. West, C.-C Cheng, and B. C. Baker, *J. Electrochem. Soc.,* **145**, 3070 (1998).
2. P. C. Andricacos, C. Uzoh, J. O. Dukovic, J. Horkans, and H. Deligianni, *IBM J. Res. Dev.,* **42**, 567 (1998).
3. H. Deligianni, J. O. Dukovic, P. C. Andricacos, and E. G. Walton, in *Electrochemical Processing in ULSI Fabrication and Semiconductor/Metal Deposition II*, P. C. Andricacos, P. C. Searson, C. Reidsema-Simpson, P. Allongue, J. L. Stickney, and G. M. Oleszek, Editors, PV 99-9, p. 52, The Electrochemical Society Proceedings Series, Pennington, NJ (1999).
4. J. Reid and S. Mayer, in *Advanced Metallization Conference 1999, Proceedings of the Conference*, p. 53, MRS, Warrendale, PA (2000).
5. T. Ritzdorf, D. Fulton, and L. Chen, in *Advanced Metallization Conference 1999, Proceedings of the Conference*, p. 101, MRS, Warrendale, PA (2000).
6. E. Richard, I. Vervoort, S. H. Brongersma, H. Bender, G. Beyer, R. Palmans, S. Lagrange, and K. Maex, in *Advanced Metallization 1999, Proceedings of the Conference*, p. 149, MRS, Warrendale, PA (2000).
7. T. P. Moffat, J. E. Bonevich, W. H. Huber, A. Stanishevsky, D. R. Kelly, G. R. Stafford, and D. Josell, *J. Electrochem. Soc.,* **147**, 4524 (2000).
8. T. P. Moffat, D. Wheeler, W. H. Huber, and D. Josell, *Electrochem. Solid-State Lett.,* **4**, C26 (2001).
9. D. Josell, D. Wheeler, W. H. Huber, and T. P. Moffat, *Phys. Rev. Lett.,* **87**, 016102 (2001).
10. D. Wheeler, D. Josell, and T. Moffat, *J. Comput. Phys.*, Submitted.
11. D. Josell, D. Wheeler, W. H. Huber, J. E. Bonevich, and T. P. Moffat, *J. Electrochem. Soc.,* **148**, C767 (2001).
12. Unpublished results.